



Published in final edited form as:

J Comput Chem. 2008 March ; 29(4): 514–522. doi:10.1002/jcc.20810.

Combined QM/MM and Path Integral Simulations of Kinetic Isotope Effects in the Proton Transfer Reaction Between Nitroethane and Acetate Ion in Water

JIALI GAO^{1,2}, KIN-YIU WONG¹, and DAN T. MAJOR^{1,3}

¹ Department of Chemistry and Supercomputing Institute, University of Minnesota, 207 Pleasant Street S.E., Minneapolis, Minnesota 55455-0431

² Centro Nacional de Supercomputación, Programa Biología Computacional C/Jordi Girona 29, Barcelona 08034, Spain

³ Department of Chemistry, Bar-Ilan University, Ramat-Gan 52900, Israel

Abstract

An integrated Feynman path integral-free energy perturbation and umbrella sampling (PI-FEP/UM) method has been used to investigate the kinetic isotope effects (KIEs) in the proton transfer reaction between nitroethane and acetate ion in water. In the present study, both nuclear and electronic quantum effects are explicitly treated for the reacting system. The nuclear quantum effects are represented by bisection sampling centroid path integral simulations, while the potential energy surface is described by a combined quantum mechanical and molecular mechanical (QM/MM) potential. The accuracy essential for computing KIEs is achieved by a FEP technique that transforms the mass of a light isotope into a heavy one, which is equivalent to the perturbation of the coordinates for the path integral quasiparticle in the bisection sampling scheme. The PI-FEP/UM method is applied to the proton abstraction of nitroethane by acetate ion in water through molecular dynamics simulations. The rule of the geometric mean and the Swain–Schaad exponents for various isotopic substitutions at the primary and secondary sites have been examined. The computed total deuterium KIEs are in accord with experiments. It is found that the mixed isotopic Swain–Schaad exponents are very close to the semiclassical limits, suggesting that tunneling effects do not significantly affect this property for the reaction between nitroethane and acetate ion in aqueous solution.

Keywords

combined QM/MM; path integral simulations; PI-FEP/UM; kinetic isotope effects; SwainSchaad exponent

Introduction

Of great interest is to accurately compute kinetic isotope effects (KIEs) for chemical reactions in solution and in enzymes because the ratio of the reaction rates between light and heavy isotopomers provides the most direct experimental probe to the nature of the transition state.

¹ This is illustrated by the work of Schramm,² who developed highly potent inhibitors to the enzyme purine nucleoside phosphorylase (PNP) based on the transition state structure derived from measured KIEs. In principle, Schramm's approach can be applied to other enzymes, but

in practice it is often limited by the lack of an adequate model to match computed and experimental KIEs. The challenge to theory is the difficulty to accurately determine the small difference in free energy of activation due to isotope replacements. This is further exacerbated by the complexity and size of an enzyme system that requires statistical averaging. In this study, we utilize an integrated path integral-free energy perturbation and umbrella sampling (PI-FEP/UM) method to assess the statistical precision for computing KIEs of condensed phase reactions.^{3,4}

Quantum mechanics is essential for computing KIEs of reactions in solutions and in enzymes.^{5,6} First, electronic structural theory is required to adequately describe the potential energy surface for bond forming and breaking processes. Secondly, nuclear quantum effects including both quantized vibration and tunneling are needed to obtain accurate rate constants. We employ a combined quantum mechanical and molecular mechanical (QM/MM) approach to represent the potential energy surface, including the electronic degrees of freedom for the reactants.^{7,8} This method has been described previously and extensively used for numerous systems in solution and in enzymes. In this article, we focus on the method for treating the nuclear quantum effects, with a specific aim of computing KIEs for condensed phase reactions.

A variety of methods have been developed to treat nuclear quantum effects for gas-phase reactions.⁹ In principle, these techniques can be directly extended to condensed phase systems; however, the size and complexity of these systems often make it intractable computationally. One method that has been successfully introduced to the study of enzyme reaction rates is the ensemble-averaged variational transition state theory with QM/MM sampling (EA-VTST-QM/MM),^{5,6} which has been applied to a number of enzyme systems. This technique includes multidimensional tunneling. In another work, a grid-based hybrid approach was used to model nuclear quantum effects by numerically solving the vibrational wavefunction of the quantized nucleus.¹⁰ The latter method is somewhat difficult to extend the method to quantize more than one particle because of increased computational costs.¹¹

The discretized Feynman path integral method has been used in a variety of applications in solution and biological systems.^{12–20} It offers an efficient and general approach for treating nuclear quantum effects in condensed phase simulations. In particular, the centroid path integral molecular dynamics method provides a conceptual framework for estimating the quantum mechanical free energy of activation,^{21,22} but it is computationally expensive for modeling large systems such as enzymes, especially if combined QM/MM potentials are used to represent the potential energy surface. An alternative procedure is to carry out classical molecular dynamics simulations first, followed by centroid path integral simulations to determine the quantum effects. Sprik et al.¹⁵ explored this idea to estimate quantum effects for an electron in a lattice matrix of hard spheres, whereas Warshel and coworkers^{23–26} employed a quantized classical path (QCP) method in several applications to determine quantum effects along a reaction path. In the QCP method, the classical potential of mean force (PMF) is obtained first, followed by estimating quantum contributions to the free energy of activation. The most significant feature of these studies is that classical and quantum simulations are fully separated, making it particularly attractive and efficient for enzymatic reactions.

Recently, we developed a computational procedure, called BQCP,²⁷ by extending the bisection sampling method developed by Ceperley for free particle sampling to centroid path integral simulations.^{28,29} The excellent convergence behavior of the BQCP method, coupled with a FEP approach, has enabled us to obtain converged results in computed KIEs through a series of validation studies.^{3,4,30,31} In this article, we further examine the performance of this PI-FEP/UM method to investigate the primary and secondary KIEs in the reaction of nitroethane and acetate ion in water.

In the following we first summarize the theoretical background, followed by computational details. Then, results and discussions are presented. The study is concluded with highlights of main findings.

Theoretical Background

Path Integral Quantum Mechanical Rate Theory

The discretized Feynman path integrals provide a powerful approach to treat quantum effects in chemical reactions in condensed phases.^{12–14,16–23} This arises from the isomorphism of the discretized path integral and a classical partition function for a system of polymer quasiparticles,¹³ which are connected harmonically with its neighbors, and have coordinates $\mathbf{r}_i^{(n)}$ corresponding to the imaginary time slices $\tau_i = (i - 1)\hbar\beta/P$. A key concept in path integral quantum mechanical transition state theory (QTST) is the centroid variable in path integration,^{16,18,21,22,32–34} defined as the geometrical center of the quasiparticles:

$$\bar{\mathbf{r}}^{(n)} = \frac{1}{P} \sum_{i=1}^P \mathbf{r}_i^{(n)} \quad (1)$$

where the superscript (n) specifies the n th quantized atom. The discretization parameter P is chosen to be sufficiently large such that the numerical results converge to the quantum limit. In this approach, the quantum mechanical equilibrium properties as well as the free energy are obtained from the classical averages for a fictitious system governed by the effective potential^{12,13}

$$V_{\text{eff}}[\{\mathbf{r}_i^{(n)}\}, \mathbf{S}] = \sum_{n=1}^N \frac{\pi P}{\beta \lambda_n^2} \sum_i^P (\mathbf{r}_i^{(n)} - \mathbf{r}_{i+1}^{(n)})^2 + \frac{1}{P} \sum_i^P U(\mathbf{r}_i^{(1)}, \dots, \mathbf{r}_i^{(N)}, \mathbf{S}) \quad (2)$$

where N is the number of quantized atoms, $\mathbf{r}_i^{(n)}$ is the position of quasiparticle i of atom n with $\mathbf{r}_1^{(n)} = \mathbf{r}_{P+1}^{(n)}$, \mathbf{S} represents all coordinates of classical particles, $U(\mathbf{r}_i^{(1)}, \dots, \mathbf{r}_i^{(N)}, \mathbf{S})$ is the potential of the system, and $\beta = 1/k_B T$ with k_B being Boltzmann's constant and T the temperature. In eq. (2), $\lambda_n = (2\pi\beta\hbar^2/M_n)^{1/2}$ is the de Broglie thermal wavelength of atom n of a mass M_n . The dynamics generated by the effective potential of eq. (2) has no physical significance; it is merely used as a procedure to obtain the correct ensemble of configurations.

The most important feature of the path integral quantum transition state theory is that it is expressed analogously to the classical TST, including a quantum activation term and a dynamical correction factor.^{16,34,35} According to this view, the central quantity in determining the quantum transition rate is governed by the free energy of activation for the centroid reaction coordinate $z[\mathbf{F}]$, and the QTST rate constant is given by

$$k_{\text{QTST}} = \frac{1}{2} \langle |\dot{z}| \rangle_{z^\ddagger} e^{-\beta w(z^\ddagger)} / \int_{-\infty}^{z^\ddagger} dz e^{-\beta w(z)} \quad (3)$$

where $w(z)$ is the PMF as a function of the centroid reaction coordinate $z[\mathbf{F}]$, z^\ddagger is the value of the centroid reaction coordinate at the maximum of the PMF, and $\langle |\dot{z}| \rangle_{z^\ddagger} = (2/\pi\beta M_{\text{eff}})^{1/2}$ is a

dynamical frequency factor approximated by the velocity for a free particle of effective mass M_{eff} along the reaction coordinate $z[\mathbf{r}]$ direction. The exact quantum mechanical rate constant is obtained by multiplying the QTST rate constant by a correction factor or transmission coefficient κ ³⁵:

$$k = \kappa \cdot k_{\text{QTST}} \quad (4)$$

Although the expressions of eqs. (3) and (4) have identical forms to that of the classical rate constant, unlike classical variational transition state theory, there is no variational upper bound in the QTST rate constant because the quantum transmission coefficient κ may be either greater than or less than one. Equation (3) was initially derived with the assumption of a planar dividing surface along a rectilinear reaction coordinate. Messina et al.³⁴ described a generalization of the dividing surface, which may depend both on the centroid coordinates and on its momenta. Unfortunately, there is no simple Jacobian-like correction that can be used for the transformation from a locally rectilinear reaction coordinate to the curvilinear reaction coordinate. A variational approach has been developed to optimize the generalized dividing surface to yield the minimum value of the QTST rate constant,³⁴ though the optimal rate is not an upper bound.

There is no practical procedure to compute the quantum transmission coefficient κ in eq. (4). For a model reaction with a parabolic barrier along the reaction coordinate coupled to a bath of harmonic oscillators, the quantum transmission coefficient is the Grote–Hynes (GH) classical transmission coefficient, κ_{GH} .^{16,36} Often, the classical κ is used to approximate the quantum transmission coefficient; however, there is no correspondence between classical and quantum dynamic trajectories and the effects of tunneling may greatly affect reaction dynamics near the barrier top.

As in classical TST, the PMF, $w(z)$, can be computed from the equilibrium average without any dynamical information, and it is defined by

$$e^{-\beta[w(z) - w(z_{\text{R}})]} = e^{-\beta\Delta F(z)} = \frac{\langle \delta(z[\bar{\mathbf{r}}] - z) \rangle}{\langle \delta(z[\bar{\mathbf{r}}] - z_{\text{R}}) \rangle} \quad (5)$$

where z_{R} is the minimum point at the reactant state in the PMF and the ensemble average $\langle \dots \rangle$ is obtained by the effective potential of eq. (2). Equation (5) also serves as a definition of the path integral centroid free energy, $\Delta F(z)$, at z relative to that at the reactant state minimum. Note that the inherent nature of quantum mechanics is at odds with a PMF as a function of a finite reaction coordinate. Nevertheless, the reaction coordinate function $z[\mathbf{r}]$ can be evaluated from the path centroids $\bar{\mathbf{r}}$,^{18,24,34,35} first recognized by Feynman and Hibbs¹² as the most classical-like variable in quantum statistical mechanics and later used by Gilan and many others in practice.¹⁸ Studies have shown that the activation free energy in the centroid path integral QTST “captures most of the tunneling and quantization effects”; which give rise to deviations from classical TST.^{37–40}

It is also useful to rewrite eq. (3) as follows

$$k_{\text{QTST}} = \frac{1}{\beta h} e^{-\beta\Delta F_{\text{CPI}}^{\ddagger}} \quad (6)$$

where the path integral centroid free energy of activation $\Delta F_{\text{CPI}}^{\ddagger}$ is defined by

$$\Delta F_{\text{CPI}}^{\ddagger} = \Delta F(z^{\ddagger}) + F_{\text{CPI}}^{\text{R}} \quad (7)$$

and

$$F_{\text{CPI}}^{\text{R}} = \frac{1}{\beta} \ln \frac{1}{\lambda_{\text{eff}}} \int_{-\infty}^{z^{\ddagger}} dz e^{-\beta[\Delta F(z)]} \quad (8)$$

$F_{\text{CPI}}^{\text{R}}$ corresponds to the free energy of the system in the reactant (R) state region relative to the lowest point, which may be interpreted as the entropic contributions or motions correlating with the progress coordinate z . λ_{eff} is the de Broglie thermal wavelength of the centroid reaction coordinate with an effective mass M_{eff} at the dividing surface, which is determined in the centroid path transition state ensemble.

Centroid Path Integral Simulations

For simplicity, we consider a system of a single quantized particle in a classical environment; thus, the superscript specifying quantum atoms coordinates [eq. (1)] has been dropped. The quantized nucleus is represented by a ring of P quasiparticles, whose coordinates are denoted as $\mathbf{r} \equiv \{\mathbf{r}_i, i = 1, \dots, P\}$, with a definition of $\mathbf{r}_{P+1} = \mathbf{r}_1$. The canonical QM partition function of the hybrid system can be written as follows:

$$Q_p^{\text{qm}} = \frac{1}{\Omega} \int d\mathbf{S} \int d\bar{\mathbf{r}} \left(\frac{P}{\lambda_M^2} \right)^{3P/2} \int d\mathbf{R} e^{-\beta V_{\text{eff}}(\{\mathbf{r}\}, \mathbf{S})} \quad (9)$$

where Ω is the volume element of classical particles, $V_{\text{eff}}(\{\mathbf{r}\}, \mathbf{S})$ is the effective quantum mechanical potential specified in eq. (2), and $\int d\mathbf{R} = \int d\mathbf{r}_1 \dots \int d\mathbf{r}_P \delta(\mathbf{r})$. The key result in the hybrid classical and path integral approach¹⁵ or QCP^{24,25} is that the quantum partition function can be rewritten as the double averages^{3,4,15,24-27}:

$$Q_{\text{qm}} = Q_{\text{cm}} \langle \langle e^{-\beta \Delta \bar{U}(\bar{\mathbf{r}}, \mathbf{S})} \rangle_{FP, \bar{\mathbf{r}}} \rangle_U \quad (10)$$

where Q_{cm} is the classical partition function defined in ref. ¹², the average $\langle \dots \rangle_U$ is a purely classical ensemble average obtained according the potential $U(\bar{\mathbf{r}}, \mathbf{S})$, and the inner average $\langle \dots \rangle_{FP, \bar{\mathbf{r}}}$ represents a path-integral free-particle sampling, carried out without the external potential $U(\bar{\mathbf{r}}, \mathbf{S})$ ^{4,24,25}:

$$\langle \dots \rangle_{FP, \bar{\mathbf{r}}} = \frac{\int d\mathbf{R} \{ \dots \} e^{-(\pi P / \lambda_M^2) \sum_i^P (\Delta \mathbf{r}_i)^2}}{\int d\mathbf{R} e^{-(\pi P / \lambda_M^2) \sum_i^P (\Delta \mathbf{r}_i)^2}} \quad (11)$$

where $\Delta \mathbf{r}_i = \mathbf{r}_i - \mathbf{r}_{i+1}$. In eq. (10), the average potential energy is given as follows

$$\Delta\bar{U}(\bar{\mathbf{r}}, \mathbf{S}) = \frac{1}{P} \sum_i^P \{U(\mathbf{r}_i, \mathbf{S}) - U(\bar{\mathbf{r}}, \mathbf{S})\} \quad (12)$$

This double-averaging procedure was used by Sprik et al.¹⁵ for a system consisting of one electron embedded in random hard spheres. Hwang and Warshel^{24,25} extensively exploited this idea for studying quantum effects in condensed phase reactions. Hwang and Warshel^{24,25} used an approach called QCP, in which the classical simulations and quantum corrections are fully separated.^{26,41} The expression of eq. (10) is particularly useful because the quantum free energy of the system can be obtained first by carrying out classical trajectories according to the classical distribution, $\exp[-\beta U(\mathbf{r}, \mathbf{S})]$, and then, by determining the quantum contributions through free particle sampling based on the distribution

$\exp[-\beta(\pi P/\beta\lambda_M^2) \sum_i^P (\Delta\mathbf{r}_i)^2]$. This double averaging yields the exact path integral centroid density.^{4,15,24,25}

On the basis of eq. (10), the path integral PMF, defined as a function of the centroid reaction coordinate, \bar{z} , can be readily expressed by:

$$e^{-\beta w(\bar{z})} = e^{-\beta w_{cm}(\bar{z})} \langle \delta(z=\bar{z}) \langle e^{-\beta \Delta\bar{U}(\bar{z}[\mathbf{r}], \mathbf{S})} \rangle_{FP, \bar{z}} \rangle_U \quad (13)$$

where $w(\bar{z})$ $w_{cm}(\bar{z})$ are the centroid quantum mechanical and the classical mechanical PMF, respectively, and the average potential energy $\Delta\bar{U}(\bar{z}[\mathbf{r}], \mathbf{S})$ is given in eq. (12).

A bisection sampling scheme has been developed for centroid path integral simulations,^{3,27} based on the original procedure of Ceperley,²⁹ and this method (BQCP) has been implemented in the context of the QCP simulation.²⁴ Through a series of investigations,^{30,31} it has been demonstrated that the BQCP sampling procedure yields rapidly converging results,^{3,27} which has been a major problem for application to enzymes. In BQCP sampling, any particle position of the cyclic quasiparticles can be expressed as⁴

$$\mathbf{r}_i = \sqrt{2\pi\lambda_M} \boldsymbol{\theta}_i; \quad i=1, 2, \dots, P \quad (14)$$

where the vector $\boldsymbol{\theta}_i$ is a generalized position vector, properly scaled, generated randomly according to the free particle distribution, and associated with earlier levels of bisection sampling. The specific details have been given in refs. ^{3,4}, and ²⁷. Note that the beads positions are dependent on the particle mass via λ_M .

Kinetic Isotope Effects

Sequential Centroid Path Integral and Umbrella Sampling (PI/UM) Method—

Using eq. (6), the KIEs between a light isotope L and a heavy isotope H can be computed by

$$\text{KIE} = \frac{k^L}{k^H} = e^{-\beta[\Delta F^L(\bar{z}_L^*) - \Delta F^H(\bar{z}_H^*)]} e^{-\beta(F_{CPL}^R(\bar{z}_L^R) - F_{CPL}^R(\bar{z}_H^R))} \quad (15)$$

where \bar{z}_L^\neq , \bar{z}_H^\neq , \bar{z}_L^R , and \bar{z}_H^R are, respectively, the values of the centroid reaction coordinate at the transition state and reactant state minimum for the light and heavy isotopes in the centroid path-integral PMF, $w(\bar{z}) = -k_B T \ln Q_{\text{qm}}(\bar{z})$ [see also eq. (13)], and $F_{\text{CPL}}^R(\bar{z}_L^R)$ and $F_{\text{CPL,H}}^R(\bar{z}_H^R)$ are the free energies defined by eq. (8) for the two isotopes, respectively. The latter quantities are the free energies of the system in the reactant well relative to its minimum and the transition frequency at the centroid transition state. Here, we use the reactant minimum free energies for the two isotopes to approximate the reactant state free energies. Thus, eq. (15) shows that the two potentials of mean force can be determined separately for the *L* and *H* isotopes using umbrella sampling simulations along the centroid reaction coordinate (PI/UM),^{3,4} and this is, in deed, what is typically done. However, the statistical fluctuations in the actual simulation for computing the PMF is as large as the isotope effect itself, resulting in poor convergence.

Integrated Centroid Path Integral-Free Energy Perturbation and Umbrella Sampling (PI-FEP/UM) Method

An alternative approach is to obtain the ratio of the quantum partition functions for two different isotopes directly through FEP theory over the mass from light to heavy isotopes in one simulation.⁴ Specifically, we have developed an integrated path integral-free energy perturbation and umbrella sampling (PI-FEP/UM) method for computing KIEs, in which molecular dynamics simulations are first carried out to obtain the classical mechanical PMF using umbrella sampling.^{47,48} Then, the nuclear coordinates of atoms associated with the chemical reaction are quantized by a path integral with the constraint that the centroid positions coincide with their corresponding classical coordinates. KIEs are evaluated by FEP between heavy and light atom masses, which is related to the quantized quasiparticle positions. In this approach, the KIE is expressed as follows:

$$\text{KIE} = \frac{k^L}{k^H} = \left[\frac{Q_{\text{qm}}^L(\bar{z}_L^\neq)}{Q_{\text{qm}}^H(\bar{z}_H^\neq)} \right] \left[\frac{Q_{\text{qm}}^H(\bar{z}_H^R)}{Q_{\text{qm}}^L(\bar{z}_L^R)} \right] e^{-\beta(F_{\text{CPL}}^R(\bar{z}_L^R) - F_{\text{CPL,H}}^R(\bar{z}_H^R))} \quad (16)$$

Considering an atom transfer reaction where the light atom of mass M_L is replaced by a heavier isotope of mass M_H , we use exactly the same sequence of random numbers, *i.e.*, displacement vectors, to generate the bisection path integral distribution for both isotopes in order to obtain the free particle distribution. Thus, the resulting coordinates of these two bead-distributions are related by the ratio of the corresponding masses:

$$\frac{\mathbf{r}_{i,L}}{\mathbf{r}_{i,H}} = \frac{\lambda_{M_L} \boldsymbol{\theta}_i}{\lambda_{M_H} \boldsymbol{\theta}_i} = \sqrt{\frac{M_H}{M_L}}; \quad i=1, 2, \dots, P \quad (17)$$

where $\mathbf{r}_{i,L}$ and $\mathbf{r}_{i,H}$ are the coordinates for bead *i* of the corresponding light and heavy isotopes.

By substituting the integration variable for the heavy isotope quasiparticle coordinates in eq. (13) by the relationship of eq. (17), we can obtain the ratio of the two isotopic partial quantum partition functions at a given reaction coordinate value \bar{z} (centroid coordinates) exactly by the following FEP⁴:

$$\frac{Q_{\text{qm}}^H(\bar{z})}{Q_{\text{qm}}^L(\bar{z})} = \frac{\langle \delta(z - \bar{z}) \langle e^{-\frac{\beta}{P} \sum_i \Delta U_i^{L \rightarrow H}} e^{-\beta \Delta \bar{U}_L} \rangle_{\text{FP,L}} \rangle_U}{\langle \delta(z - \bar{z}) e^{-\beta [F_L(\bar{z}, \mathbf{S}) - F_{\text{FP}}^0]} \rangle_U} \quad (18)$$

where the superscripts or subscripts L and H specify computations done using light and heavy isotopes, $\Delta\bar{U}_L$ is defined by eq. (12), F_{fp}^0 is the free energy of the free particle reference state for the quantized particles,¹² and $\Delta U_i^{L\rightarrow H} = U(\mathbf{r}_{i,H}) - U(\mathbf{r}_{i,L})$ represents the difference in “classical” potential energy at the heavy and light bead positions $\mathbf{r}_{i,H}$ and $\mathbf{r}_{i,L}$. In eq. (18), we obtain the free energy (inner average) difference between the heavy and light isotopes by carrying out the bisection path integral sampling with the light atom and then perturbing the heavy isotope positions according to eq. (17). Then, the free energy difference between the light and heavy isotope ensembles is weighted by a Boltzmann factor for each quantized configuration (outer average). The statistical errors, computed by dividing the entire simulations into 10 blocks and their 10 separate averages, for the computed KIEs using the PI-FEP/UM approach are significantly smaller than that from PI/UM calculations.

Computational Details

Potential Energy Function

In the present study, we use a combined QM/MM potential in molecular dynamics simulations,^{7,42} in which the solute is represented explicitly by an electronic structure method and the solvent is approximated by the three-point charge TIP3P model for water.⁴³ The details have been described in a number of articles. In the deprotonation of nitroethane by acetate ion, the standard semiempirical AM1 model⁴⁴ failed to yield adequate energetic results. Consequently, a set of specific reaction parameters (SRP) has been developed within the AM1 formalism to fit results from high-level *ab initio* theory as well as from experiments.^{4,30} The performance of the SRP-AM1 model has been reported previously, and we focus here on the study of the KIEs using the PI-FEP/UM method.

Simulation Details

All simulations are performed using periodic boundary conditions in the isothermal-isobaric (NPT) ensemble at 25°C and 1 atm. A total of 898 water molecules were included in a cubic box of about $30 \times 30 \times 30 \text{ \AA}^3$. The solute molecules are treated quantum-mechanically. Nonbonded electrostatic interactions are described by the particle-mesh Ewald summation method for QM/MM simulations,⁴⁵ whereas van der Waals interactions are smoothed to zero at 9.5 Å based on group–group separations. The bond lengths and angles of solvent water molecules are constrained by the SHAKE algorithm, and an integration step of 1 fs was used for all calculations.⁴⁶

The PMF profile is obtained using the umbrella sampling technique.⁴⁷ In this approach, the reaction is divided into a series of segments called simulation “windows,” in which a biasing potential is applied to allow sufficient sampling of high-energy regions along the reaction pathway. The effect of the biasing potential is subsequently removed when the separate simulation windows are combined to produce the overall PMF by using the weighted histogram analysis method.⁴⁸ For the proton transfer reaction, the classical reaction coordinate is defined as the difference in distance for the proton between the donor (α carbon of nitroethane) and the acceptor (an oxygen of the acetate ion) atom: $Z_{\text{PT}} = r(\text{C}_\alpha - \text{H}) - r(\text{H} - \text{O})$. In the current simulations, 32 windows have been employed. To start the simulations, the system is slowly heated to the target temperature over the course of 25 ps, and thereafter equilibrated for 100–200 ps. Subsequently, each window is further equilibrated for 25–50 ps before data collection commenced. Each window is sampled for ca. 100–150 ps, totaling ca. 4 ns for the deprotonation reaction.

The BQCP simulations employed 29,168 classical configurations for each isotope (^1H , ^2H , and ^3H ; or H, D, and T), combined with 10 path-integral steps per classical step. For the deprotonation reaction the nitroethane C_α -atom, the abstracting acetate oxygen, the

transferring proton, as well as the secondary hydrogen atom, are quantized. Each quantized atom has spawned into 32 beads.

To estimate statistical uncertainties in the computed KIEs, the entire path integral simulations have been divided into 10 segments, each of which is treated as independent simulations. Standard uncertainties ($\pm 1\sigma$) were determined from the total average and those from the 10 separate blocks. All simulations employed the CHARMM program⁴⁹ and all path-integral simulations used a parallel version that efficiently distributes integral calculations for the quantized beads.

Results and Discussion

Deprotonation of Nitroethane by Acetate Ion in Water

The proton abstraction reaction of nitroalkane by acetate ion has been extensively studied in physical organic chemistry, which shows an unusual Brønsted relationship in water, known as the nitroalkane anomaly.^{50–52} Furthermore, there is significant solvent effects on the proton transfer reaction, raising the barrier by 16 kcal/mol in water relative to that for the gas phase reaction from the ion-dipole complex.⁵⁰ This process is also catalyzed by nitroalkane oxidase in the initial step of the oxidation of nitroalkanes.⁵³ For the enzymatic process, the deprotonation step by Asp402 is rate-limiting with nitroethane as the substrate. Recently, Valley and Fitzpatrick determined the KIEs for the dideuterated substrate [1,1-²H₂]nitroethane in nitroalkane oxidase, and the proton/deuteron abstraction reaction by an acetate ion in water in the absence of a catalyst. In the enzyme-catalyzed reaction the KIE was found to be 9.2 ± 0.4 , whereas in aqueous solution the KIE was measured to be 7.8 ± 0.1 .⁵⁴ We have previously studied the solvent effects on the proton transfer reaction of nitroethane and acetate ion and reported the preliminary results of H/D KIEs.³⁰ Here, we report the KIEs for all D and T primary and secondary isotope effects and provide a detailed analysis of their relationships.

In the present study, we employ a reparameterized semiempirical model using the AM1 formalisms, and this SRP model (specific reaction parameters) was fitted to the Gaussian3 results, and the details of the SRP parameterization procedure have been described previously.³⁰ The aim here is to examine our PI-FEP/UM method for KIE calculations, but we emphasize that the SRP model is a good one, and the computed energy of reaction for the proton abstraction of nitroethane by acetate is 8.7 kcal/mol, in adequate accord with the G3 result of 10.3 kcal/mol. The classical PMF for the deprotonation of nitroethane by acetate is presented in Figure 1. The computed barrier is 27.4 kcal/mol, while the computed free energy of reaction is 7.1 kcal/mol, slightly higher than the corresponding experimental values of 24.8 and 5.2 kcal/mol, respectively.^{4,30,54}

Since light atoms are involved in the proton abstraction reaction, quantization of the “primary” and “secondary” hydrogen atoms as well as the donor carbon atom and acceptor oxygen atom has a major impact on the computed free energy of activation, by lowering the barrier height by 3.0 kcal/mol for the proton transfer reaction relative to the classical barrier in Figure 1. Thus, the estimated free energy of activation is 24.4 kcal/mol, in accord with the experimental value of 24.8 kcal/mol.^{4,54} This result illustrates the importance of including nuclear quantum effects to accurately determine the free energy of activation for proton transfer reactions.⁵⁵

H/D and H/T Kinetic Isotope Effects

The computed primary and secondary KIEs for D and T substitutions are listed in Table 1. Figures 2–6 depict the computed ratios of the partial quantum partition functions as a function of the centroid path integral reaction coordinate. The KIEs have been computed without including the free energy difference given in eq. (8), which may introduce some errors in the

present calculations. Their effects will be analyzed in the future by devising a practical computational approach to examine this quantity. To directly compare the computed KIE with experiment, which employed the dideuterated compound, 1,1- $^2\text{H}_2$ [nitroethane], we also made the same substitutions in our computation at the $\text{C}\alpha$ -position.⁵⁴ Throughout this paper, we use the convention that the subscript of a rate constant specifies the primary isotope and the superscript defines the secondary isotope. When two isotopes are given sequentially in figures and captions (e.g., XX), the first denotes the primary and the second letter specifies the secondary isotope.

The computed H/D primary and secondary intrinsic KIEs are $k_{\text{H}}^{\text{H}}/k_{\text{D}}^{\text{H}}=6.63 \pm 0.31$ and $k_{\text{H}}^{\text{H}}/k_{\text{H}}^{\text{D}}=1.34 \pm 0.13$, respectively, whereas the total effect where both primary and secondary hydrogen atoms are placed by a deuterium isotope is $k_{\text{H}}^{\text{H}}/k_{\text{D}}^{\text{D}}=8.31 \pm 1.13$ (Table 1), which may be compared with the experimental value of 7.8.⁵⁴ There are no experimental data for comparison with the results of single site substitutions. The computational results allow us to examine the rule of the geometric mean (RGM),⁵⁶ which is expressed as follows:

$$k_{\text{H}}^{\text{H}}/k_{\text{D}}^{\text{H}}=k_{\text{H}}^{\text{D}}/k_{\text{D}}^{\text{D}}=\frac{(k_{\text{H}}^{\text{H}}/k_{\text{D}}^{\text{D}})}{(k_{\text{H}}^{\text{H}}/k_{\text{H}}^{\text{D}})} \quad (19)$$

The RGM states that there is no isotope effect from a second site on the KIE of the first site.⁵⁷ The rule was originally derived at high temperature limit with small quantum tunneling corrections,⁵⁶ and it has been shown to have negligible deviations on model systems using semiclassical transition state theory.⁵⁸ However, deviations or the observations of RGM breakdown are often used as a measure of the extent of tunneling in the system.⁵⁷ Using the RGM of eq. (19), we obtain an estimated value of 8.88 (6.63×1.34) for the total deuterium KIE if the free energies of the primary and secondary KIE were additive. This gives a ratio of 1.07 over the actual computed value (8.31). Another way of interpreting the results is that there is a secondary KIE of 1.07 on the primary KIEs:

$$s_{\text{HD}}=\frac{(k_{\text{H}}^{\text{H}}/k_{\text{D}}^{\text{H}})}{(k_{\text{H}}^{\text{D}}/k_{\text{D}}^{\text{D}})}=\frac{6.630}{(8.308/1.340)}=1.07 \quad (20)$$

This result indicates that there is some correlation in the motions between the secondary hydrogen and the primary hydrogen in the proton transfer reaction between nitroethane and acetate ion in water.

Primary and secondary tritium KIEs are also given in Table 1, which have values of $k_{\text{H}}^{\text{H}}/k_{\text{T}}^{\text{H}}=12.96 \pm 0.98$ and $k_{\text{H}}^{\text{H}}/k_{\text{H}}^{\text{T}}=1.38 \pm 0.18$. These effects are greater than the deuterium KIEs because of its larger mass. Employing the rule of the geometric mean, an estimated total tritium KIE of $k_{\text{H}}^{\text{H}}/k_{\text{T}}^{\text{T}}=17.8$ is obtained.

Swain–Schaad Exponents

Following the notation used by Huskey,⁵⁷ the single site Swain–Schaad exponents,⁵⁹ which relate the H/T isotope effect with that of the H/D or the D/T ratio, are given by

$$n_{\text{HD}} = \frac{\ln(k_{\text{H}}^{\text{H}}/k_{\text{T}}^{\text{H}})}{\ln(k_{\text{H}}^{\text{H}}/k_{\text{D}}^{\text{H}})} \quad \text{and} \quad (21\text{a})$$

$$n_{\text{DT}} = \frac{\ln(k_{\text{H}}^{\text{H}}/k_{\text{T}}^{\text{H}})}{\ln(k_{\text{D}}^{\text{H}}/k_{\text{T}}^{\text{H}})} \quad (21\text{b})$$

Here, it is assumed that the isotope effects are determined solely by the use of one-frequency model with contributions only from the zero-point energy without tunneling. Studies have shown that the value of n_{HD} for primary KIEs is typically in the range of 1.43–1.45.⁵⁷ Although the n_{HD} value for secondary KIEs is not as well established, a similar value seems also to be valid. Deviations from these values are thought to be indications of contributions from tunneling.⁶⁰ Using the data in Table 1, we obtained a single-site Swain–Schaad exponent of $n_{\text{HD}}^{(1)}=1.35$ for the primary KIE, and of $n_{\text{HD}}^{(2)}=1.09$ for the secondary KIE. The exponents, $n_{\text{DT}}^{(1)}$ and $n_{\text{DT}}^{(2)}$, for D/T ratios are 3.82 and 12.3, respectively. These values show significant deviations from the semiclassical limits, particularly on secondary KIEs, which can have greater computational errors because of the small free energy difference. It appears that the deviations may be attributed to a too large secondary H/D effect.

In general, it is more sensitive use mixed isotopic Swain–Schaad exponent to assess tunneling contributions⁵⁹:

$$n_{\text{DT}}^{\text{DD}} = \frac{\ln(k_{\text{H}}^{\text{H}}/k_{\text{T}}^{\text{H}})}{\ln(k_{\text{D}}^{\text{D}}+k_{\text{T}}^{\text{D}})} \quad \text{and} \quad (22\text{a})$$

$$n_{\text{DT}}^{\text{DT}} = \frac{\ln(k_{\text{H}}^{\text{H}}/k_{\text{H}}^{\text{T}})}{\ln(k_{\text{D}}^{\text{D}}/k_{\text{D}}^{\text{T}})} \quad (21\text{b})$$

The first equation is the primary Swain–Schaad exponent, which describes the relationship between H/T primary KIE when the secondary position is occupied by a hydrogen atom with the D/T primary KIE when the secondary position is occupied by a deuterium isotope. The second equation describes a similar relationship for the secondary KIEs. Values of the mixed Swain–Schaad exponents significantly greater than 3.3 are typically attributed to contributions from tunneling,⁶⁰ and experimental studies showed that the secondary exponent is more sensitive than the primary exponent in this type of analysis.

For the proton transfer reaction between nitroethane and acetate ion in water, we obtain a primary KIE Swain–Schaad exponent of $n_{\text{DT}}^{\text{DD}}=3.31$ and a secondary exponent of $n_{\text{DT}}^{\text{DT}}=3.31$. These results are close to the semiclassical limit, suggesting that tunneling contributions are not significant for this reaction in aqueous solution. To assess the tunneling contributions, we have used the multidimensional tunneling (MT) algorithm developed by Truhlar and coworkers,⁹ extended to enzyme applications in the EA-VTST method,^{5,6} to determine the average tunneling transmission factor, yielding a value of $\langle\kappa\rangle = 1.3$ using the present potential.³⁰ This suggests that tunneling only makes minor contributions in the present case for the aqueous reaction. Thus, the EA-VTST/MT results are consistent with the present PI-FEP/UM

simulations, which do not separate zero-point energy and tunneling contributions. It will be interesting to examine the effects of the enzyme active site on tunneling and the Swain–Schaad exponents.^{53,54}

Concluding Remarks

We presented a method for computing KIEs of chemical reactions in condensed phases. This method, which is abbreviated as PI-FEP/UM, integrates nuclear quantum effects obtained from Feynman path integral and FEP between different masses of two isotopes with classical PMF along the reaction coordinate determined by molecular dynamics umbrella sampling simulations. In the present study, both nuclear and electronic quantum effects are explicitly treated for the reacting system. The nuclear quantum effects are represented by bisection sampling centroid path integral simulations, while the potential energy surface is described by a combined QM/MM potential. The accuracy essential for computing KIEs is achieved by a FEP technique that transforms the mass of a light isotope into a heavy one. The PI-FEP/UM method is applied to the proton abstraction of nitroethane by acetate ion in water through molecular dynamics simulations. The rule of the geometric mean and the Swain–Schaad exponents for various isotopic substitutions at the primary and secondary sites have been examined. For the deuterium KIEs, the RGM is close to one with a computed value of 1.07. Using the RGM, we estimate that the total tritium KIE is 17.8 employing the respective pure primary and secondary KIE values. It was found that the single-site Swain–Schaad exponents are more sensitive for the secondary effects because of their small values that demand high accuracy. We found that the mixed isotopic Swain–Schaad exponents are very close to the semiclassical limits, suggesting that tunneling effects do not significantly disturb this property for the reaction in aqueous solution.

Acknowledgments

Contract/grant sponsor: National Institutes of Health; contract/grant number: GM46736

J.G. is grateful to Professor Modesto Orozco for his hospitality during a sabbatical leave at the Barcelona Supercomputing Center; he acknowledges partial support from Ministerio de Educación y Ciencia, España.

References

1. Kohen, A.; Limbach, HH., editors. *Isotope Effects in Chemistry and Biology*. Taylor and Francis Group, CRC Press; New York: 2005.
2. Schramm VL. *Acc Chem Res* 2003;36:588. [PubMed: 12924955]
3. Major DT, Garcia-Viloca M, Gao J. *J Chem Theory Comput* 2006;2:236.
4. Major DT, Gao J. *J Chem Theory Comput* 2007:3.
5. Gao J, Truhlar DG. *Annu Rev Phys Chem* 2002;53:467. [PubMed: 11972016]
6. Pu J, Gao J, Truhlar DG. *Chem Rev* 2006;106:3140. [PubMed: 16895322]
7. Gao, J. In *Reviews in Computational Chemistry*. Lipkowitz, KB.; Boyd, DB., editors. Vol. 7. VCH; New York: 1995. p. 119
8. Gao J. *Acc Chem Res* 1996;29:298.
9. Fernandez-Ramos A, Miller JA, Klippenstein SJ, Truhlar DG. *Chem Rev* 2006;106:4518. [PubMed: 17091928]
10. Hammes-Schiffer S. *Curr Opin Struct Biol* 2004;14:192. [PubMed: 15093834]
11. Wang Q, Hammes-Schiffer S. *J Chem Phys* 2006;125:184101. [PubMed: 17115732]
12. Feynman, RP.; Hibb, AR. *Quantum Mechanics and Path Integrals*. McGraw-Hill; New York: 1965.
13. Chandler D, Wolynes PG. *J Chem Phys* 1981;74:4078.
14. Berne BJ, Thirumalai D. *Annu Rev Phys Chem* 1986;37:401.
15. Sprik M, Klein ML, Chandler D. *Phys Rev B* 1985;31:4234.

16. Voth GA, Chandler D, Miller WH. *J Chem Phys* 1989;91:7749.
17. Lobaugh J, Voth GA. *Chem Phys Lett* 1992;198:311.
18. Gillan MJ. *Philos Mag A* 1988;58:257.
19. Tuckerman ME, Marx D. *Phys Rev Lett* 2001;86:4946. [PubMed: 11384388]
20. Hinsen K, Roux B. *J Chem Phys* 1997;106:3567.
21. Voth GA. *Adv Chem Phys* 1996;93:135.
22. Cao J, Voth GA. *J Chem Phys* 1994;101:6184.
23. Hwang JK, Chu ZT, Yadav A, Warshel A. *J Phys Chem* 1991;95:8445.
24. Hwang JK, Warshel A. *J Phys Chem* 1993;97:10053.
25. Hwang JK, Warshel A. *J Am Chem Soc* 1996;118:11745.
26. Feierberg I, Luzhkov V, Aqvist J. *J Biol Chem* 2000;275:22657. [PubMed: 10801792]
27. Major DT, Gao J. *J Mol Graph Model* 2005;24:121. [PubMed: 15936231]
28. Pollock EL, Ceperley DM. *Phys Rev B* 1984;30:2555.
29. Ceperley DM. *Rev Mod Phys* 1995;67:279.
30. Major DT, York DM, Gao J. *J Am Chem Soc* 2005;127:16374. [PubMed: 16305206]
31. Major DT, Nam K, Gao J. *J Am Chem Soc* 2006;128:8114. [PubMed: 16787057]
32. Gillan MJ. *Phys Rev Lett* 1987;58:563. [PubMed: 10034973]
33. Gehlen JN, Chandler D, Kim HJ, Hynes JT. *J Phys Chem* 1992;96:1748.
34. Messina M, Schenter GK, Garrett BC. *J Chem Phys* 1993;98:8525.
35. Voth GA. *J Phys Chem* 1993;97:8365.
36. Grote RF, Hynes JT. *J Chem Phys* 1981;74:4465.
37. Makarov DE, Topaler M. *Phys Rev E: Stat Phys Plasmas Fluids Relat Interdiscip Top* 1995;52:178.
38. Messina M, Schenter GK, Garrett BC. *J Chem Phys* 1995;103:3430.
39. Mills G, Schenter GK, Makarov DE, Jonsson H. *Chem Phys Lett* 1997;278:91.
40. Jang S, Voth GA. *J Chem Phys* 2000;112:8747. Erratum: 2001, 114, 1944.
41. Villa J, Warshel A. *J Phys Chem B* 2001;105:7887.
42. Gao J, Xia X. *Science* 1992;258:631. [PubMed: 1411573]
43. Jorgensen WL, Chandrasekhar J, Madura JD, Impey RW, Klein ML. *J Chem Phys* 1983;79:926.
44. Dewar MJS, Zoebisch EG, Healy EF, Stewart JJP. *J Am Chem Soc* 1985;107:3902.
45. Nam K, Gao J, York DM. *J Chem Theory Comput* 2005;1:2.
46. Allen, MP.; Tildesley, DJ. *Computer Simulation of Liquids*. Oxford University Press; Oxford: 1987.
47. Valleau, JP.; Torrie, GM. In *Modern Theoretical Chemistry*. Berne, BJ., editor. Vol. 5. Plenum; New York: 1977. p. 169
48. Kumar S, Bouzida D, Swendsen RH, Kollman PA, Rosenberg JM. *J Comput Chem* 1992;13:1011.
49. Brooks BR, Bruccoleri RE, Olafson BD, States DJ, Swaminathan S, Karplus M. *J Comput Chem* 1983;4:187.
50. Bernasconi CF. *Acc Chem Res* 1992;25:9.
51. Bordwell FG, Boyle WJ Jr. *J Am Chem Soc* 1972;94:3907.
52. Kresge A. *Can J Chem* 1974;52:1897.
53. Valley MP, Fitzpatrick PF. *Biochemistry* 2003;42:5850. [PubMed: 12741843]
54. Valley MP, Fitzpatrick PFJ. *Am Chem Soc* 2004;126:6244.
55. Garcia-Viloca M, Alhambra C, Truhlar DG, Gao J. *J Chem Phys* 2001;114:9953.
56. Bigeleisen J. *J Chem Phys* 1955;23:2264.
57. Kohen, A.; Limbach, HH., editors. *Huskey In Isotope Effects in Chemistry and Biology*. Vol. 4. Taylor and Francis; Boca Raton, FL: 2006. p. 1285
58. Saunders WH Jr. *J Am Chem Soc* 1985;107:164.
59. Swain CG, Stivers EC, Reuwer JF, Schaad LJ. *J Am Chem Soc* 1958;80:558.
60. Cha Y, Murray CJ, Klinman JP. *Science* 1989;1243:1325. [PubMed: 2646716]

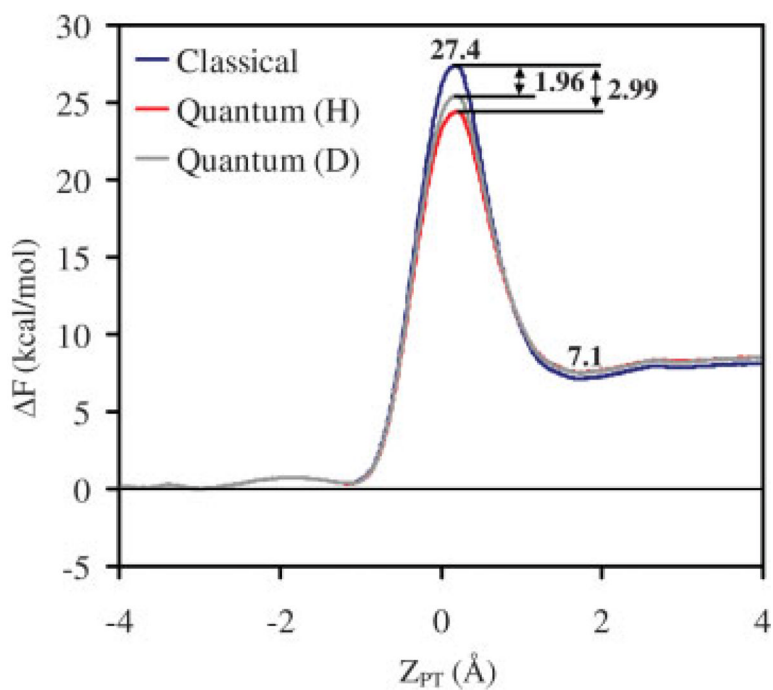


Figure 1. Computed classical and centroid path integral potentials of mean force for the proton transfer reaction between nitroethane and acetate ion in water at 25°C. The centroid path integral PMF for deuterium substitutions both at the primary and secondary sites is also shown. The reaction coordinate is defined as $Z_{PT} = r(C_{\alpha} - H) - r(H - O)$ in angstroms, where $r(C_{\alpha} - H)$ and $r(H - O)$ are distances of the transferring proton from the donor and acceptor atoms, respectively.

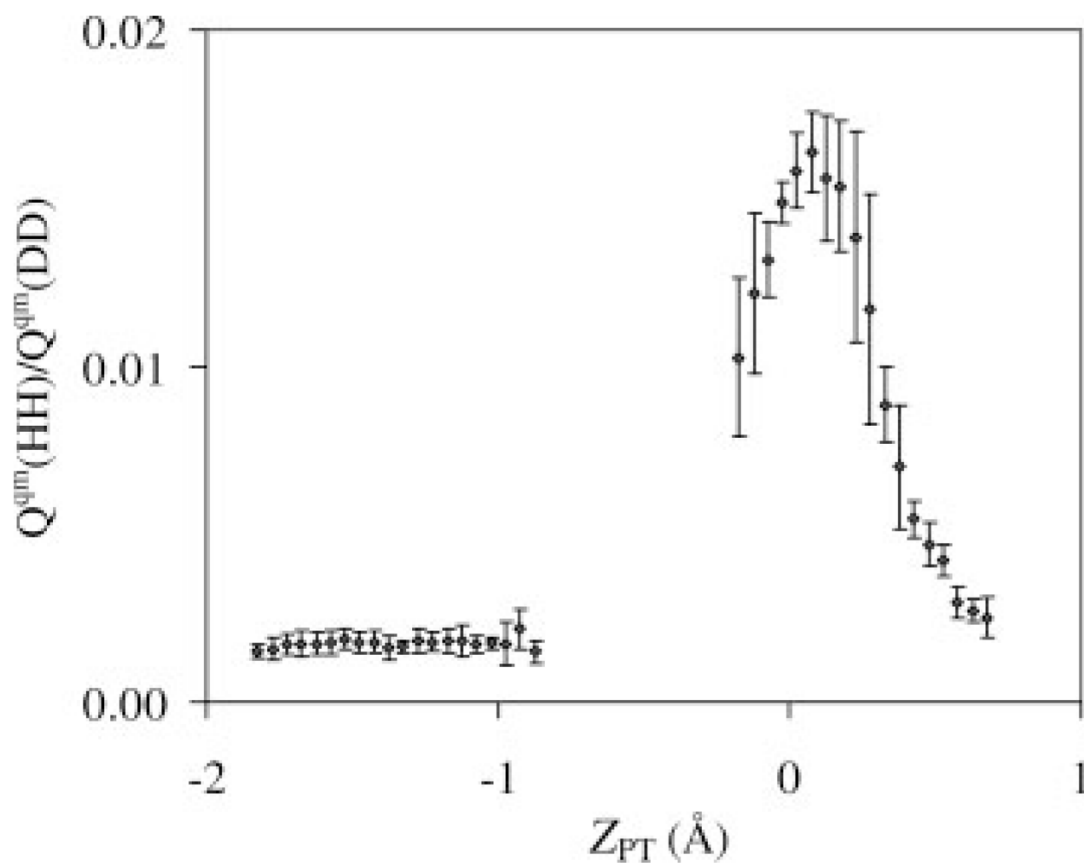


Figure 2. The ratio of the total quantum mechanical partition functions between HH and DD isotopes as a function of the reaction coordinate. In this notation, the first letter specifies the primary site and the second letter denotes the secondary site.

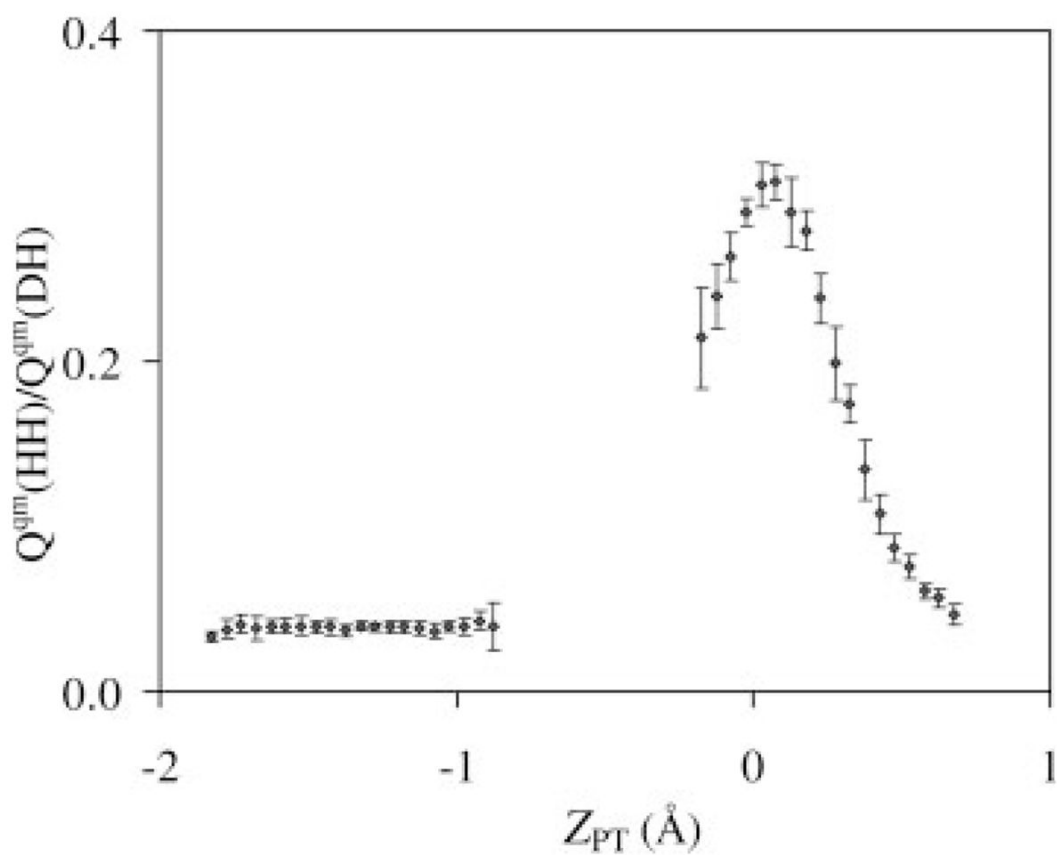


Figure 3. The ratio of the quantum mechanical partition functions as a function of the reaction coordinate for the primary H/D isotope effects in which the secondary site is occupied by a hydrogen.

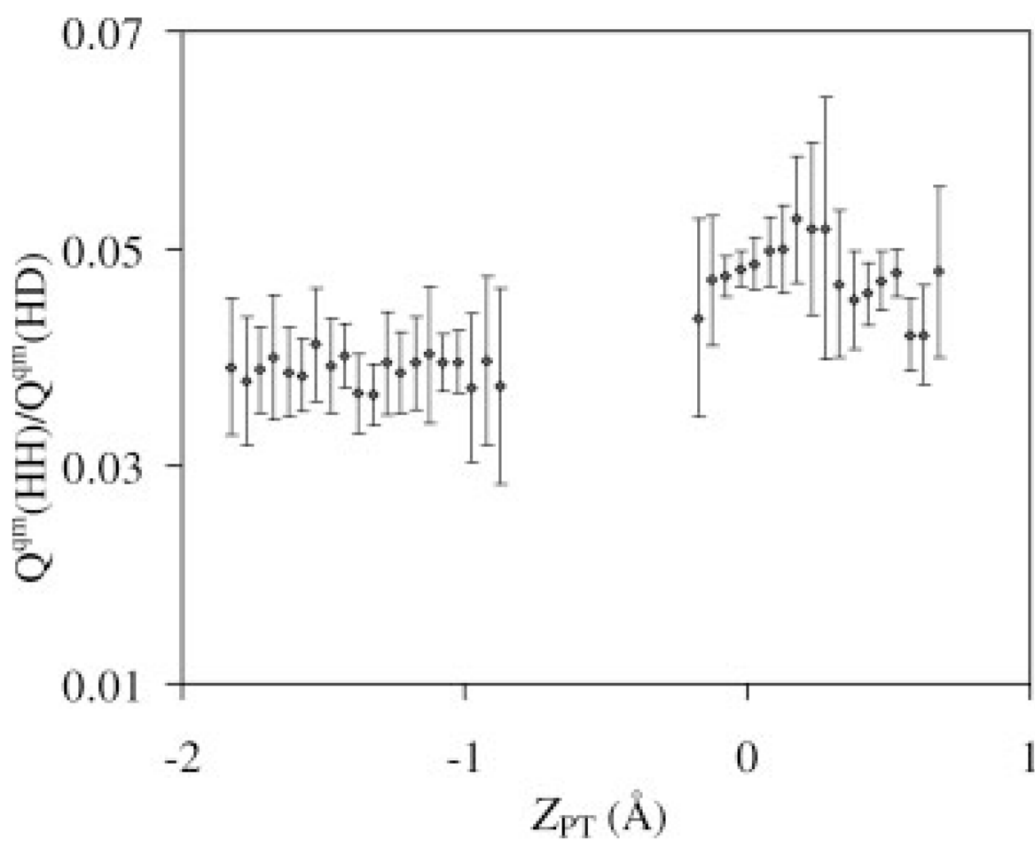


Figure 4. The ratio of the quantum mechanical partition functions as a function of the reaction coordinate for the secondary H/D isotope effects in which the primary site is occupied by a hydrogen.

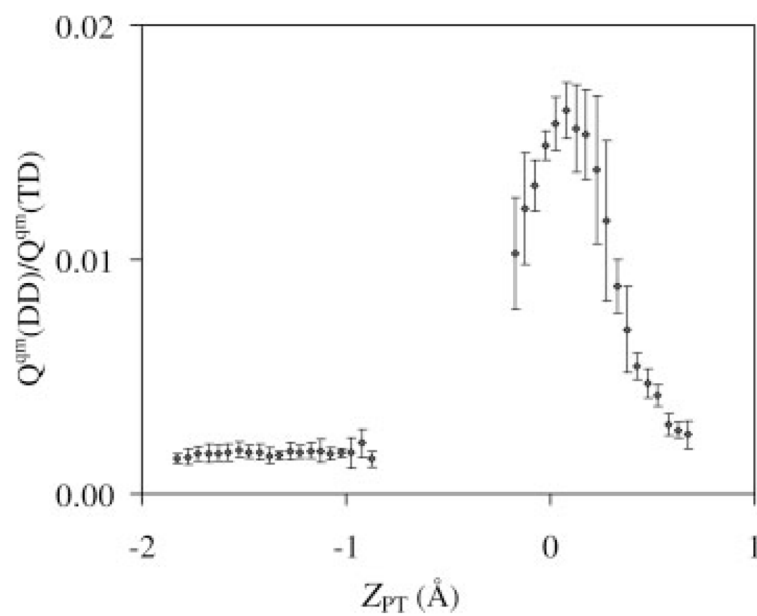


Figure 5. The ratio of the quantum mechanical partition functions as a function of the reaction coordinate for the primary D/T isotope effects in which the secondary site is occupied by a deuterium isotope.

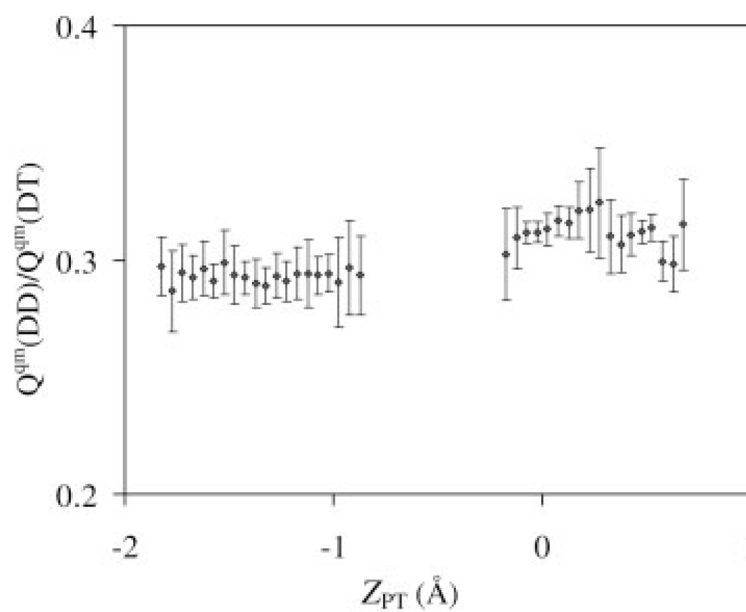


Figure 6. The ratio of the quantum mechanical partition functions as a function of the reaction coordinate for the secondary D/T isotope effects in which the primary site is occupied by a deuterium.

Table 1

Computed and Experimental Primary and Secondary Kinetic Isotope Effects for the Proton Transfer Reaction Between Nitroethane and Acetate Ion in Water at 25°C.^a

KIE	PI-FEP/UM	Expt. ^b
Primary KIE		
$k_{\text{H}}^{\text{H}}/k_{\text{D}}^{\text{H}}$	6.63 ± 0.31	
$k_{\text{H}}^{\text{H}}/k_{\text{T}}^{\text{H}}$	12.96 ± 0.98	
$k_{\text{D}}^{\text{D}}/k_{\text{T}}^{\text{D}}$	2.17 ± 0.04	
Secondary KIE		
$k_{\text{H}}^{\text{H}}/k_{\text{H}}^{\text{D}}$	1.34 ± 0.13	
$k_{\text{H}}^{\text{H}}/k_{\text{H}}^{\text{T}}$	1.38 ± 0.18	
$k_{\text{D}}^{\text{D}}/k_{\text{D}}^{\text{T}}$	1.10 ± 0.04	
Total KIE		
$k_{\text{H}}^{\text{H}}/k_{\text{D}}^{\text{D}}$	8.31 ± 1.13	7.8 ± 0.1

^a Kinetic isotope effects are determined by using the average value of the top two bins in the potential of mean force for the ratio of the partial quantum partition function for the transition state, and the average value of the middle fifteen bins for the reactant state. The bin size used for data collection is 0.05 Å in the reaction coordinate, half which may be considered as the error in the reaction coordinate value.

^b Ref. 54.